UDK 669.71:620.1./.2
Original scientific article/Izvirni znanstveni članek

ISSN 1580-2949
MTAEC9, 42(3)111(2008)

THE ACTION OF A LASER ON AN ALUMINIUM TARGET

OBSEVANJE ALUMINIJASTE TARČE Z LASERJEM

Višnja Henč-Bartolić[1], Tonica Bončina[2], Suzana Jakovljević[3], Davor Pipić[1], Franc Zupanič[2]

[1]Faculty of Electrical Engineering and Computing, University of Zagreb, Unska 3, 10000 Zagreb, Croatia
[2]Faculty of Mechanical Engineering, University of Maribor, Smetanova 17, 2000 Maribor, Slovenia
[3]Faculty of Mechanical Engineering and Naval Architecture, University of Zagreb, I. Lučića 1, 10000 Zagreb, Croatia
visnja.henc@fer.hr

Prejem rokopisa – received: 2007-08-08; sprejem za objavo – accepted for publication: 2008-02-05

A nitrogen laser beam (337 nm, 6 ns (FWHM), (3.2 ± 0.2) mJ) was focused with a quartz lens (f = 100 mm) onto an aluminium target in air at normal pressure. The laser irradiation and plasma explosion caused a modification to the Al surface and the deposition of a thin film (droplets) onto a glassy carbon plate. The irradiated target and the deposited material were studied with a scanning electron microscope (SEM) and a focused-ion-beam (FIB) device. A crater surrounded by a rim was produced on the spot of maximum irradiation on the aluminium target. The crater, very deep in comparison to its width and thickness, was presumably caused by the Kelvin-Helmholtz and the Rayleigh-Taylor instabilities. The temperatures of the electron and the massive particles were explained.

Key words: aluminium, laser ablation, thin film deposition, instabilities, temperatures

Žarek laserske svetlobe (337 nm, 6 ns ((FWHM), (3.2 ± 0.2) mJ) smo s kremenovo lečo (f = 100 mm) fokusirali na aluminijevo tarčo, ki je bila na zraku pri normalnem zračnem tlaku. Obsevanje z laserjem in eksplozija plazme sta povzročila spremembo površine aluminija ter nanos tanke plasti in kapljic na steklasto ogljikovo ploščico. Obsevano tarčo in nanesen material smo raziskali z vrstičnim elektronskim mikroskopom (SEM) in s fokusiranim ionskim curkom (FIB). Na aluminijevi tarči je na najbolj obsevanem mestu nastal krater, ki je bil zelo globok v primerjavi z njegovo širino in debelino. Krater bil povzročen zaradi Kelvin-Helmholtzove in Rayleigh-Taylorjeve nestabilnosti. V delu smo razložili tudi temperaturo elektronov in temperaturo masivnih delcev.

Ključne besede: aluminij, laserska ablacija, nanašanje tanke plasti, nestabilnosti, temperatura

1 INTRODUCTION

The laser irradiation of a target has wide applications; some examples include pulsed-laser deposition [1,2], nanoparticle manufacturing [3], and the analysis of solid materials [4,5]. It is important to reduce the plume's kinetic energy by means of a buffer gas [6] to attain a better quality of the deposited film. In this experiment we used the pulsed-laser deposition of Al droplets in air at normal pressure. It is known that the laser's interaction with matter causes melting and evaporation of the target material. Additionally, laser beams ionize the material when the power flux is sufficiently high (>1 MW/cm^2). The result is the creation of a plasma plume near the target surface. The aim of this research was to study the irradiated aluminium surface and the plasma deposit on the glassy carbon plate.

2 EXPERIMENTAL SET-UP

In the present experiment we used a pure (99.9 %) Al specimen as the target, which was irradiated with a nitrogen laser emitting pulses of 6-ns duration with an average pulse energy of (3.2 ± 0.2) mJ and a wavelength of 377 nm. The laser caused a major modification to the target surface, characteristic for these types of devices. The laser radiation was focused with a quartz lens (f = 100 mm) perpendicularly onto the aluminium target surface that was placed in air at normal pressure (**Figure 1**). The modified surface, i.e., the crater, where the irradiation and laser ablation were a maximum, was examined with a scanning electron microscope (SEM) and with a focused-ion-beam (FIB) device. The emitted plumes, a consequence of the laser ablation, were laterally deposited on the glassy carbon plate (**Figure 1**) and analyzed with the SEM.

2.1 Characteristics of the Al target

An aluminium sample of 1 cm × 1 cm × 0.3 cm was mechanically polished and cleaned with an ultrasonic device. The purity of the sample was 99.9 %. Before the laser-beam irradiation, the subsurface microstructure of the target was observed (**Figure 2**) by means of a FIB device. The small black dots (diameter ≈ 100 nm) could be explained in terms of pores. Also, the EDS analysis (**Table 1**) shows the areas of the intermetallic phases (B_1, B_2 on **Figure 2**) between Al, Fe and Si. Both appearances made stronger, deeper damage to the target during the irradiation with the laser beam. Otherwise, the UV nitrogen laser beam is absorbed in a very shallow region near the irradiated spot. The subsurface area of the Al sample was deformed due to machining. How-

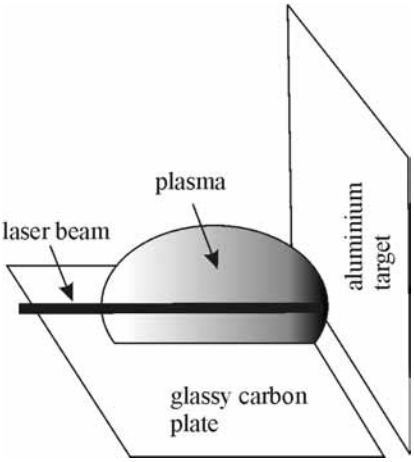

Figure 1: Target position. Relative position of Al target, carbon plate and laser beam
Slika 1: Položaj tarče. Relativen položaj aluminijeve tarče, ogljikove ploščice in laserskega žarka

ever, a thin layer of recrystallized grains could be seen on the surface.

2.2 The target after irradiation

The laser-beam energy density on the aluminium target was not uniform over the cross-section of the focal spot [7]. The damage to the aluminium after irradiation with 3, 50 and 100 laser pulses with a repetition in frequency of 1 Hz were inspected in the area of the craters and on the parts in the direct vicinity of the maximum irradiation.

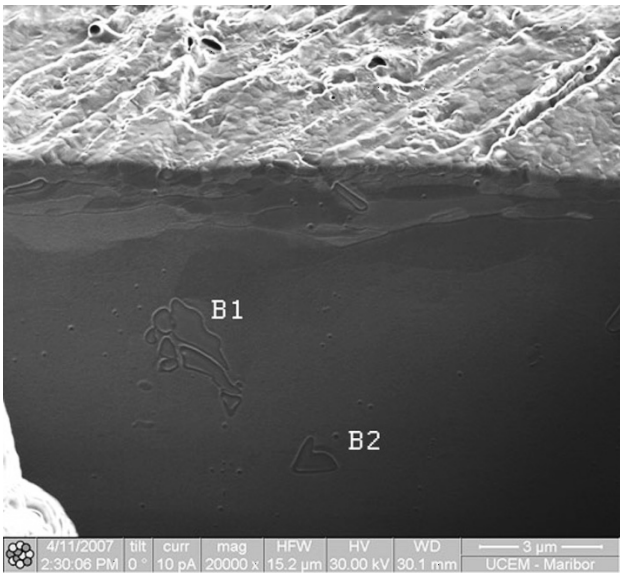

Figure 2: An overview of the Al surface and the direct area under the surface before irradiation with the laser beam. A thin and partly recrystallized surface layer is visible.
Slika 2: Pogled na površino Al in območja tik pod površino pred obsevanjem z laserskim žarkom. Viden je tanka površinska plast, ki je delno rekristalizirana

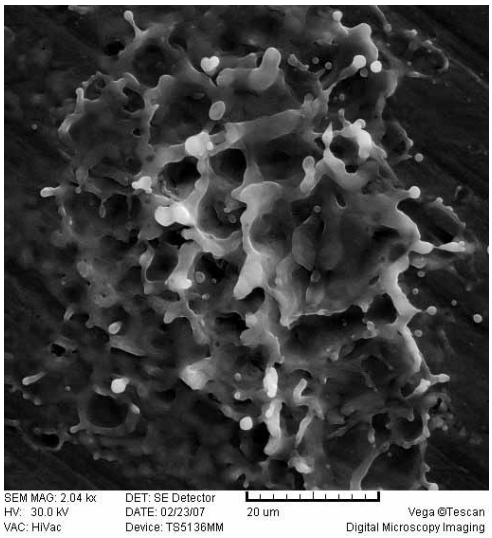

Figure 3: The target after three pulses (central part of the damage – maximum radiation) (SEM)
Slika 3: Tarča po treh impulzih (najbolj poškodovano območje, največje obsevanje žarčenje) (SEM)

The next three figures show the damage to the Al surface investigated by using the SEM. After three pulses (**Figure 3**) the target shows a melted surface as a consequence of the capillary waves. The "vertical" columns of relief, which appear due to Kelvin-Helmholtz instability, were observed. These occur at the interference between two layers, i.e., when the vapour velocity becomes much higher than the velocity of the liquid layer [8]. Therefore, the emission of droplets with radii between 0.1 µm and 0.5 µm is observed. **Figure 4** shows a deep crater formed on the target after 50 pulses. Additionally, a crater ring and a vortex formation of a self-organized closed loop of a vortex filament can be seen.

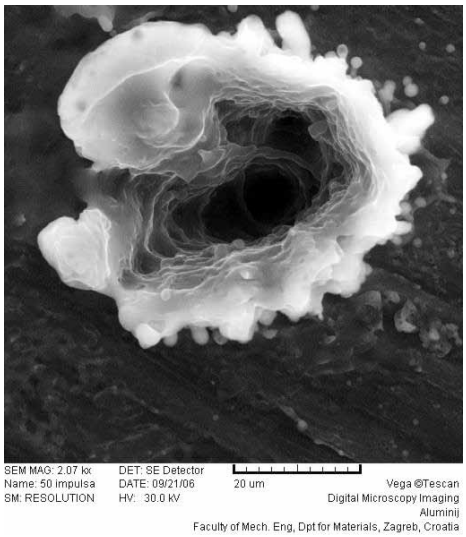

Figure 4: The target after 50 pulses (central part of damage) (SEM)
Slika 4: Tarča po petdesetih impulzih (najbolj poškodovano območje) (SEM)

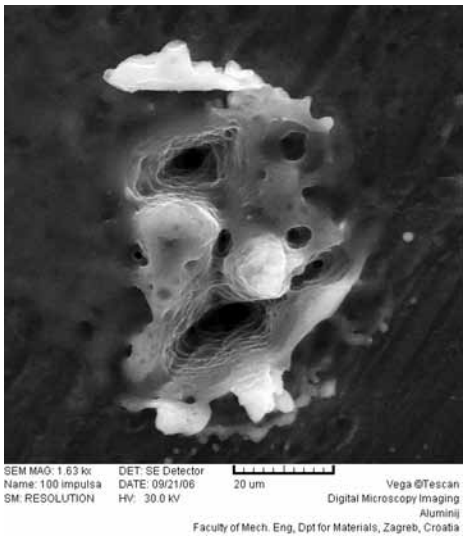

Figure 5: The target after 100 pulses (central part of damage) (SEM)
Slika 5: Tarča po stotih impulzih (najbolj poškodovano območje) (SEM)

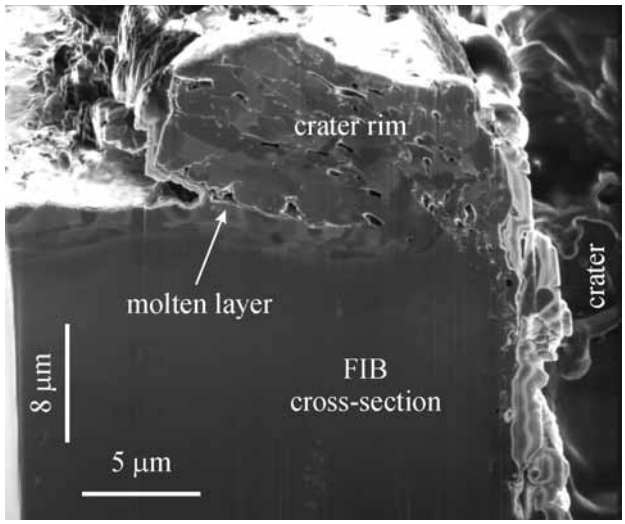

Figure 7: The Rayleigh-Taylor instability is visible on the side of the "deep" crater
Slika 7: Na stranici "globokega" kraterja je vidna Rayleigh-Taylorjeva nestabilnost

Furthermore, the crater formed after 100 pulses is shown in **Figure 5**. The crater rim is partially pushed away due to the pressure of the surrounding air and the laser-produced plasmas.

The FIB device was also used for the analysis of the laser ablation of the aluminium target situated in the air. After 50 pulses the damage at a depth of about 30 µm below the sample surface is shown in **Figures 6 and 7**. The vortex formation (**Figure 4**) and the crater configuration were caused by the Kelvin-Helmholtz and the Rayleigh-Taylor instabilities [8]. This process is analogous to the dense droplets that are instilled in the thin fluid. In other words, we take it that the laser pulses are like electromagnetic shots (or droplets). Each laser shot melts the aluminium and transforms it in a bulk, over vapour, mostly in a hot ionized gas (plasma), which is spread in all directions with a temperature gradient due to the developed plasma pressure. The distribution of the temperature establishes two types of hydrodynamic phenomena: one type in the "vertical" plane, i.e., the Kelvin-Helmholtz instability, and the other in the "horizontal" plane. The horizontal acceleration of the particles is the largest in the inner part and it decreases towards the periphery. The solidified gas builds a characteristic inner crater wall (**Figure 7**) and the vortices are the result. The gas also overheads the crater and builds the rim on the top. The gas and its

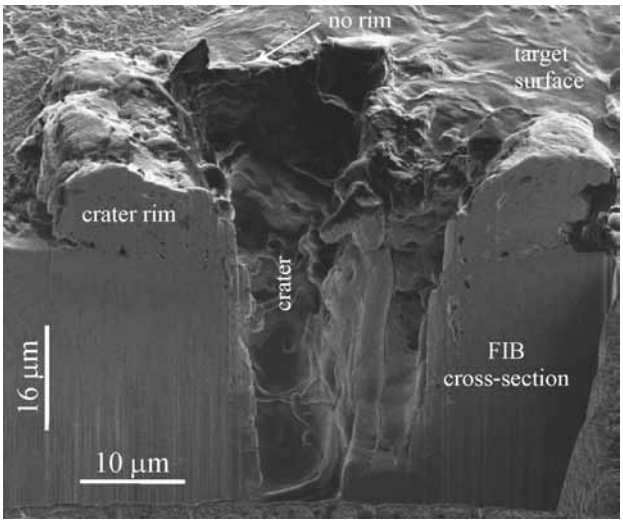

Figure 6: The Al crater after 50 pulses (FIB). Note that the length scale in the "horizontal" and "vertical" directions is not the same because the ion beam scanned the cross-section at an angle of 52°
Slika 6: Krater na aluminijevi tarči po petdesetih impulzih (FIB). Skali v vodoravni in navpični smeri nista enaki, ker je ionski curek skeniral prečni prerez pod kotom 52°

Figure 8: The traces of deposited plasma visible on the smooth glassy carbon plate
Slika 8: Na gladki steklasti ogljikovi ploščici so vidni sledovi nanosa plazme

Table 1: EDS Analysis. All elements analysed (Normalized)
Tabela 1: EDS-analiza

	Al	Si	Fe
Spectrum 1 / B1	64.90	4.42	30.69
Spectrum 2 / B2	71.93	4.05	24.03

All results in mass fraction (%)

Table 2: Aluminium Al
Tabela 2: Aluminij Al

Atomic mass	26.98
1. Ionization potential	5.999 eV
2. Ionization potential	18.83 eV
Heat of fusion	10.79 kJ/cal
Heat of vaporization	293.40 kJ/mol

conversions into droplets have been partly thrown out from the crater. The crater depth increases with the number of laser pulses while forming a narrow capillary. It can be concluded that the described process can be explained as a type of capillary discharge.

The particles of the bulk are ejected from the crater. They are deposited on the target surface and (**Figure 8**) on the smooth glassy carbon plate as frozen droplets. Their dimensions decrease with the distance of the crater.

2.3 Electron temperature of the aluminium plasmas

A feature of the developed plasmas, which is a consequence of the laser irradiation, is the electron temperature, T_e. For a target placed in vacuum this property was estimated using the theoretical formula known from literature [9,10]:

$$T_e/\mathrm{K} = 2.98 \cdot 10^4 \cdot A^{1/8} \, (Z+1)^{-5/8} \cdot Z^{1/4} \, (I \cdot \lambda)^{1/2} \cdot \tau^{1/4} \quad (1)$$

where A is the atomic weight of an ion, $Z = 1$ is the charge of the ion, known from a spectroscopic experiment [7]. Due to the fact that the second ionization potential of Al is $\approx$ 19 eV (**Table 2** [11]), multiple ionization has been neglected and only simple charge ions have been considered. (We found ions with the charge $Z = 2$ only in the titanium plasma produced by this nitrogen laser. The energy deposition was more effective than in other cases since the wavelength of the laser is in the vicinity of the Ti resonance lines [12]). The number density of the electrons (N_e) is equal to the number density of the ions (N_i), i.e., $N_i \approx N_e$.

In Equation (1), $\lambda = 337 \cdot 10^{-7}$ cm is the radiation wavelength, $\tau = 6 \cdot 10^{-9}$ s is the laser pulse duration and I is the absorbed laser-radiation intensity ($1.3 \cdot 10^8$ W/cm^2), reduced by about 5 %. In other words, the laser-absorbed pulse energy is released by the heat of fusion, the heat of vaporization, the ionized energy and the plasma energy. The ejected volume was evaluated from the Al target after 50 laser irradiations (pulses), as shown in **Figure 6**. Using **Table 2** the thrown mass/pulse is $\approx 1.32 \cdot 10^{-11}$. Therefore, from **Table 2**, the calculated heat of fusion is $\approx 1.4 \cdot 10^{-4}$ J/pulse, the heat of vaporization is $\approx 3.9 \cdot 10^{-6}$ J/pulse, and the ionized energy is $\approx 7.6 \cdot 10^{-6}$ J/pulse. The above-mentioned energies are about 5 % of the total pulsed-laser energy. Therefore, the laser-generated plasma converts significant amounts of the absorbed laser energy at the Al target into the energy of plasma particles.

From Equation (1) the electron temperature for the aluminium plasma with single ionized atoms is (1.4 ± 0.1) eV. This is somewhat lower than the temperature measured by means of the spectral lines [7] when the Al target is located in air at normal pressure. Furthermore, the aluminium ablation will be compared with the model prediction made by S. Amoroso [13]. The ejected mass is composed of electrons, excited neutrals, ground-state neutrals and ions. The vapour breakdown occurs within $\approx$1 ns and the electron temperature strongly increases from the low value up to a calculated 1.4 eV. The temperatures of the electrons and the massive particles become nearly the same, reaching an equilibrium condition in a time interval close to the laser-pulse duration.

3 CONCLUSION

The laser irradiation of the aluminium surface in air at normal pressure caused the modification of the target, and the explosion of plasma mixed with expanding target droplets. After a few pulses, the ablated surface shows the topology produced by the Kelvin-Helmholtz instability. Subsequent laser pulses resulted in the formation of a crater in the area irradiated by highest energy density. The crater is surrounded by a rim that was formed presumably due to the Kelvin-Helmholtz and the Rayleigh-Taylor instabilities. The rim was partly pushed away after a number of pulses, (approximately 100). The surface of the glassy carbon plate was covered by a thin aluminium film containing numerous droplets. The applied set-up shows that there is a possibility of depositing a thin film.

A small discrepancy between the theoretical electron temperature and the measured value is expected and it can be explained by the presence of air at normal pressure where the target was situated. In our earlier investigations with other targets (e.g., Ti, Cu [12,14]) we noticed that the obtained temperatures are 10 % higher than in vacuum, i.e., (1.5 ± 0.1) eV for aluminium.

Acknowledgement

The authors gratefully acknowledge the assistance that was kindly provided by Prof. H.-J. Kunze, Nikolina Volf and Iva Orhanović.

4 REFERENCES

[1] M. Von Allmen, Laser Beam Interaction with Materials, Springer, Heidelberg 1987

[2] V. Khomchenko at al. Appl. Surface Science, 247 (**2005**) 434

[3] S. S. Harilal. C. V. Bindhu. M. S. Tillack, F. Najmabadi, A. C. Garis, J. Appl. Phys. 93 (**2003**), 2380

[4] R. E. Russo, Appl. Spectrosc. 49 (**1995**), 14A

[5] I. I. Beilis, Laser and particles beams 25 (**2007**), 53

[6] R. K. Tharea, A. K. Sharma, Plasma Science, IEEE Conf. Record-Abstracts (**2004**), 263

[7] Ž. Andreić, V. Henč-Bartolić, H.-J. Kunze, Physica Scripta 48 (**1993**), 331

[8] S. Lugomer, Laser matter interaction, Profil, Zagreb 2001

[9] O.A. Novodvorsky. C. Wenzel, J.W. Bartha, O.D. Khramova, E.O. Filippova, Optics and Lasers in Engineering 36 (**2001**) 3, 303

[10] O. A. Novodvorsky, O.D. Khramova, C. Wenzel, J.W. Bartha. E.O. Filippova, J. of Appl. Phys. 94 (**2003**) 5, 3612

[11] http://pol.spurious.biz/projects/chemglobe

[12] V. Henč-Bartolić, Ž. Andreić, H.-J. Kunze, Physica Scripta 59 (**1994**), 368

[13] S. Amoruso, Appl. Phys. A 69 (**1999**) 323

[14] V. Henč-Bartolić, Ž. Andreić, M. Stubičar, H.-J. Kunze, Fizika A 7 (**1998**) 4, 205